Proceedings of ICRC 2001: 784 © Copernicus Gesellschaft 2001

ICRC 2001

Pierre Auger Atmospheric-Monitoring LIDAR System

A. Filipčič[1], D. Veberič[1], D. Zavrtanik[1], M. Zavrtanik[1], R. Cester[2], M. Mostafa[2], R. Mussa[2], and the Pierre Auger Collaboration[3]

[1]Nova Gorica Polytechnic, Vipavska 13, SI-5000 Nova Gorica, Slovenia
[2]INFN, Sezione di Torino, Via P. Giuria 1, I-10125 Torino, Italy
[3]Observatorio Pierre Auger, Av. San Martin Norte 304, (5613) Malargüe, Argentina

Abstract. Measurements of the cosmic-ray air-shower fluorescence at extreme energies require precise knowledge of atmospheric conditions. The absolute calibration of the cosmic-ray energy depends on the fluorescence absorption between its origin and point of its detection. A dedicated LIDAR prototype was constructed for on-line monitoring of the atmospheric parameters at the Pierre Auger Observatory in Argentina. The laser-backscattering method is used to parametrize attenuation length over the detection volume.

1 Introduction

The Pierre Auger Observatory (Auger, 1997; Zavrtanik, 2000) will use two techniques to measure air-showers induced by cosmic rays with energies above $10^{20} e$V. The hexagonal grid of water-Čerenkov tanks (Pryke, 1997) will sample the air-shower at ground (1500 m above the sea level), while the fluorescence detectors will detect fluorescence light produced along the air-shower volume through the atmosphere. The fluorescence yield is proportional to electromagnetic particle density and therefore provides a measure of the cosmic-ray energy. In this sense, the atmosphere can be treated as elementary-particle detector. However, the weather conditions change the atmophere transmission properties dramaticaly. Therefore, an absolute calibration system for fluorescence light absorbtion is the essential part of the fluorescence detector (Arčon, 1999; Bird, 1995).

The energy of the cosmic ray is proportional to the fluorescence yield P_0 at the place of its production. The fluorescence light traverses a specific path l from the point of origin to the point of detection at the fluorescence detector. The detected light P_d is smaller than P_0 due to absorption on molecules or aerosols in the atmosphere,

$$P_d = P_0 \int_0^l \exp\left[-\alpha(x)x\right] \mathrm{d}x, \qquad (1)$$

Correspondence to: A. Filipčič (Andrej.Filipcic@ijs.si)

where $\alpha(x)$ is the volume extinction coefficient, and is proportional to the absorption cross section and scatterer density. The integral (1) is calculated along the fluorescence light path.

The volume extinction coefficient $\alpha(x)$ has to be known over the whole detection volume of the fluorescence detector, which in the case of the Pierre Auger Observatory corresponds to the ground area of 3000 km^2 and the height of $\sim$ 15 km. One of the most suitable calibration detectors is the backscattering LIDAR system, where a short laser-light pulse is transmitted from fluorescence detector position to the atmosphere in the direction of interest. The backscattered ligh is detected with a mirror and photomultiplier tube as a function of time. If the laser light is of the same wavelength as the fluorescence light, the absorption over the path l is for a factor of 2 larger due to traversal in both directions. The LIDAR equation describes the received laser power from distance l as a function of volume extinction coefficient $\alpha(x)$ and backscattering coefficient $\beta(x)$,

$$P_r(l) = P_0 \frac{ct_0}{2} \beta(l) \frac{A_r}{l^2} \exp\left[-2\int_0^l \alpha(x)\mathrm{d}x\right]. \qquad (2)$$

P_0 is the transmitted laser power and A_r is the effective receiving area of the detector, which is a product of the area of the mirror and the overlap between its field of view with the laser beam. t_0 is pulse duration. If the signal P_r is measured over the fluorescence detection volume, α can be determined as a function of detection volume. The precision of cosmic-ray energy calibration directly depends on the measurement precision of α.

2 The LIDAR System

The LIDAR system prototype has been constructed at Nova Gorica Polytechnic in collaboration with INFN Torino. The system design is somehow specific to satisfy the needs of the Pierre Auger Observatory. It has to be steerable and able to

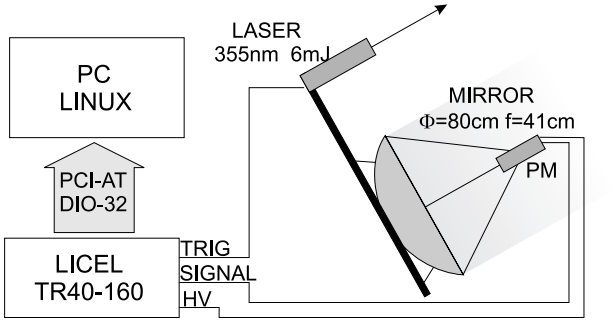

Fig. 1. Schematic view of the LIDAR system. Three mirrors of 80 cm diameter and UV-laser head are mounted on the EAS-TOP reused telescope. The LICEL TR40-160 receives the trigger from the laser and the signal from Hammamatsu R7400 phototube. The Linux-PC controls the LICEL digitizer through PCI-DIO-32HS Digital Input/Output card. The telescope motors are controlled through RS-323 port.

scan the sky fast enough to reduce the systematic errors due to atmosphere changes.

The laser is Continuum MiniLite-1 frequency tripled YaG system, which is able to trasmit up to 15 shots per second, each with energy of 6 mJ and 4 ns duration. The emitted wavelength is 355 nm which is in the $300 - 400$nm range of fluorescence spectrum. The old EAS-TOP experiment telescope was reused and remodeled by INFN Torino (Agnetta, 1996). It is able to cover $360° \times 90°$ of the sky and can move from one direction to the other in less than a minute. It has four mirror mounts, one being used for the laser head. The other three mounts have parabolic 80 cm- diameter mirrors with focal length of 41 cm. They are made of aluminum coated pyrex and protected with SiO_2. The distance between laser beam and the mirror center is about 1 m. Due to the very sensitive fluorescence detector design, the laser pulse energy should not exceed few mJ. To compensate for the small transmitted power, three large mirrors with total receiving area of 1.5 m^2 are used.

The mirrors reflect received light onto Hammamatsu R7400 photompultipler with operating voltage up to 1000 V and gain of $\sim 10^6$. To suppress background, a broadband UG-1 filter with 60% trasmitance at 353 nm and FWHM=50 nm is used.

The signal is digitized by three-channel LICEL transient recorder TR40-160 with 12 bit resolution at 40 MHz sampling rate with 16k trace length combined with 250 MHz fast photon counting system. The maximum detection distance is around 60 km. The LICEL is operated by PC-Linux system through National Instruments digital input-output card (PCI-DIO-32HS) with Comedi drivers (Comedi, 2001) and ROOT DAQ interface (ROOT, 2001).

3 LIDAR Equation Solution

The LIDAR equation has in general two unknown parameters $\alpha(x)$ and $\beta(x)$ which are both function of distance. With the system described above, the phenomenological relation

$$\beta \propto \alpha^k \tag{3}$$

fits the data very well, where k is constant (Klett, 1985a). In this case, the Klett method for inversion of the LIDAR equation (2) can be used (Klett, 1985).

$$\alpha(x) = \frac{\exp[(S(x) - S_m)/k]}{\alpha_m^{-1} + \frac{2}{k}\int_0^l \exp[(S(x) - S_m)/k]\mathrm{d}r}, \tag{4}$$

where the range-corrected signal variable is defined as $S(x) = \ln[P_r(x)x^2]$. S_m and α_m are quantities at some reference distance $x = l_m$ usually chosen as a maximal distance, where the signal is still significantly above background.

4 Test Measurements

Test measurements with the new system where performed at Pino near Torino, Italy in April 2001 in a typical city environment, where two mirrors were used. One mirror was equipped with Hammamatsu RS7400 phototube and 20 Mhz LICEL digitizer while the other used Philips 2020Q phototube and LeCroy digital osciloscope. The Hammamatsu tube was operated at ~ 700 V and Philips 2020Q at ~ 1800 V.

The range-corrected LICEL signal $P_r(l)l^2$ is shown in figure 2. For the homogeneous atmosphere ($\alpha(x) = \mathrm{const}$), which is mostly the case for horizontal measurements, the histogram should be straight line in logarithmic scale. The

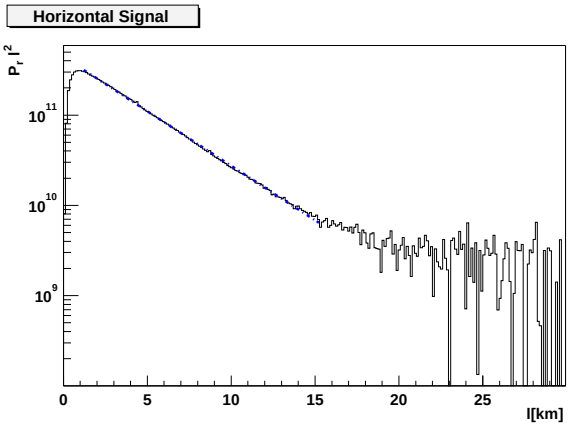

Fig. 2. Signal from LICEL Digitizer for horizontal measurement with 2000 laser shots summed. The measurement was performed at ~ 500 m above the ground during the period of 30 minutes. The straight line is an exponential fit to show the homogeneity between 1 and 15 km.

laser beam fully enters the mirrors field of view at distance ~ 1 km. Above ~ 15 km, the signal drops to the level of noise. To increase the range, the phototube operating voltage should be increased, however, the limited range of digitizer would cause the overflow for distances below 2 km.

The signal from the measurement at an inclination of $30°$ is shown in figure 3. The weather was cloudy with the cloud

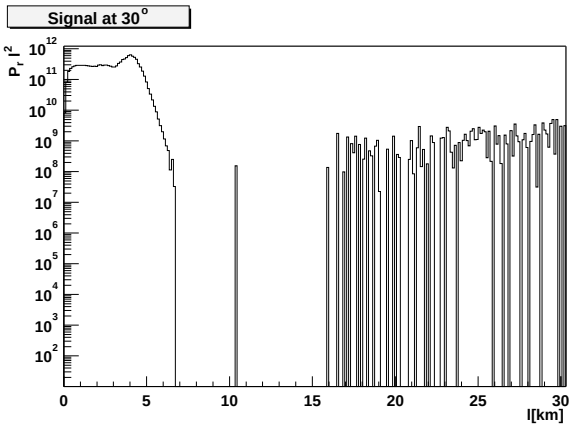

Fig. 3. Signal from LICEL Digitizer for measurement at 30° above the horizon with 2000 laser shots summed. The clouds at distances from 3 to 6 km absorb all the laser light, therefore, no signal is received from distances above ∼ 6 km. The histogram points above 6 km are due to noise.

base at height of about 2 km, so that an excess of backscattered light can be seen around distance $l = 4$ km. Above that distance there is almost no signal due to high absorption in the clouds.

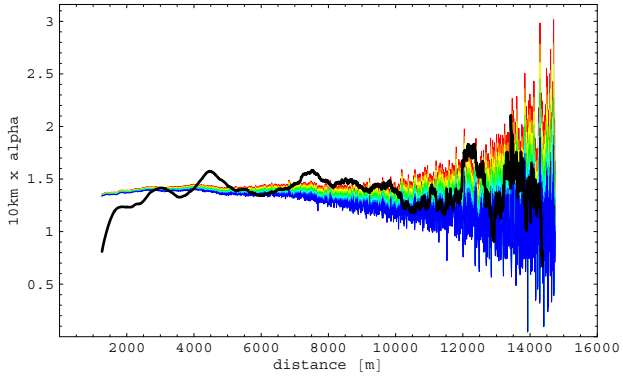

Fig. 4. Volume extinction coefficient α as a function of distance for horizontal measurement. The line corresponds to a local running slope fit of 100 neigbhouring data points, while the band of lines are Klett's solutions for different estimates α_m.

Typical values of constant k are in the range from 0.7 to 1.3 depending on aeorosol and molecule composition of the atmosphere (Klett, 1985a; Fenn, 1966; Twomey, 1965). In the present analysis the constant k was set to 1 in Eq. (3). In figure 4, the Klett's solution of horizontal measurement is shown together with a running local fit to exponential function. The reference length in Eq. (4) was set to $x_m = 15$ km and $1/\alpha_m$ was varied between 4 km and 20 km. According to the Klett's method, the equation (4) was solved from larger distances down to smaller ones. Although the initial conditions vary a lot, the solution stabilizes very quickly at smaller distances.

The analysis of measurement at inclination of 30° is shown in figure 5. In this case, the solution is extremely stable up to

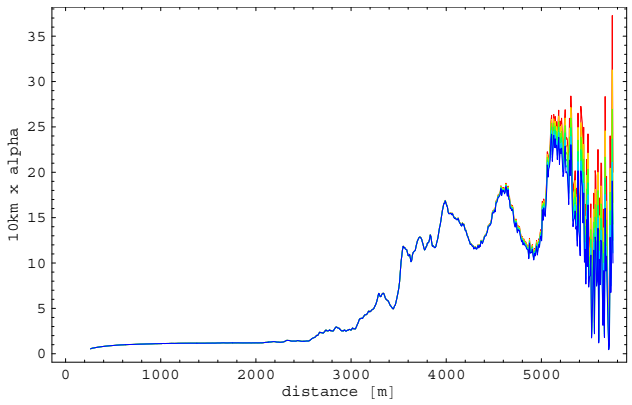

Fig. 5. Klett solution for $\alpha(x)$ as a function of distance for inclined measurement at 30°. The estimate for $1/\alpha_m$ at $x_m = 5.5$ km was varied between 400 m and 5 km. The solution bellow 5 km depends very little on the parameters α_m and S_m.

5 km, even with large variation of α_m.

The calculated optical depth

$$\tau(l) = \int_0^l \exp[-\alpha(x)x]\mathrm{d}x \qquad (5)$$

is shown in figure 6 for horizontal and inclined measurements. The upper curve corresponds to the Klett's analysis of measurement at 30°, where a dramatic increase is seen at $l = 3$ km. The two bottom curves, which are almost straight lines, correspond to horizontal measurement. The upper curve is obtained with Klett's analysis, and the bottom one is calculated from local fit to exponential. If we compare the inclined and horizontal results, the optical depth is lower for inclined measurement in the range of 1-3 km due to lower atmospheric density.

The ambiguity of initial values of S_m and α_m in Klett's equation (4) will be solved with an assumption of transverse invariance of the atmosphere. Figure 2 shows extremely good linearity up to distances of 15 km in the vicinity of an industrial city. Weather conditions in a desert-like area at the Pierre Auger Observatory site are expected to be extremely stable. The size of the area with small variation in height and no pollution sources guaranties slow changes in aerosol profile and very small fluctuations in horizontal direction. The parameter α is therefore expected to be constant in horizontal direction which fixes the value of α_m at $l = 0$. The analysis of scans over several inclinations with an assumption of horizontal invariance should give better resolution in $\alpha(x)$ and thus the optical depth. The possible horizontal fluctuations are also the outcome of the analysis which give the systematic uncertainty in the optical depth.

5 Conclusions

The prototype LIDAR system for Pierre Auger Observatory is a suitable calibration detector for parametrization of optical depth over the fluorescence detector volume. To cover the

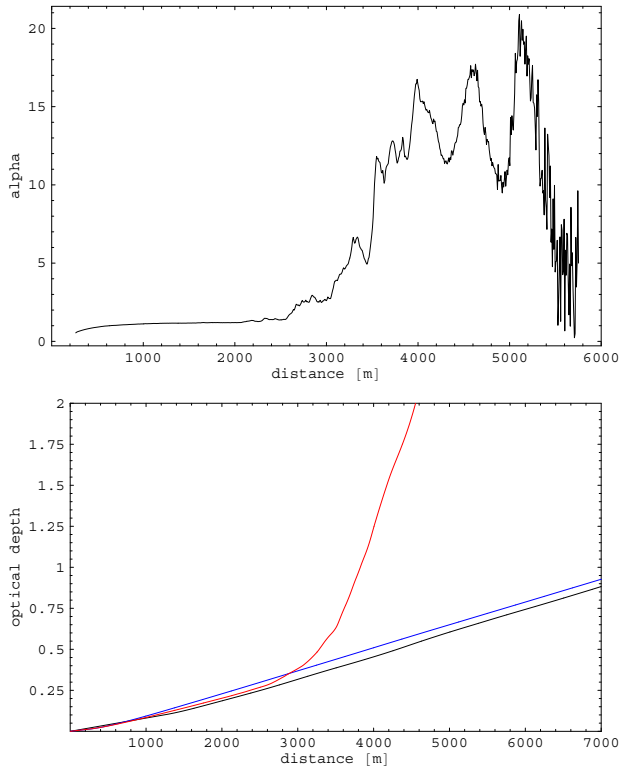

Fig. 6. Optical depth for horizontal and inclined measurements. The upper curve is for inclined measurement at 30°. The two more or less straight lines are for horizontal measurements, where the bottom one is obtained from the local fit of the slope, while the other is calculated from the Klett's solution.

whole area of the Observatory, four such systems will be deployed in the next three years. The system will perform periodical scans in all directions in parallel with fluorescence detector data taking. If the high-energy air-shower triggers the fluorescence detector, a detailed scan in its direction will be performed to minimize the systematic errors caused by local time variations of aerosol distributions. Although a detailed error analysis has still to be done, it is believed that such a system can provide the absolute energy calibration with an error bellow 5%.

References

Pierre Auger Collaboration, "Pierre Auger Project Design Report", Fermilab, 1997.

Zavrtanik, D. , "The Pierre Auger Observatory", Nucl. Phys. B (Proc. Suppl.) **85** 324–331, 2000.

Pryke, C. L. , "Simulated Performance of the Auger Observatory Water Čerenkov Arrays" Proc. 25th Int. Cosmic-Ray Conference ICRC, Durban, South Africa, July 28 - August 8, 1997, World-Scientific, Singapore **Vol. 5**, 209, 1997.

Arčon, I., Filipčič, A., and Zavrtanik, M., "UV LIDAR System for Atmospheric Monitoring and Cloud Detection",GAP-1999-028, Fermilab, 1999.

Bird, D. J. et al., "Atmospheric Monitoring for Fluorescence Detector Experiments" Proc. of 24th ICRC 95, Rome Italy,August 28 - September 8, 1995, Ed. Compositori, Bologna **Vol. 3** 560, 1995.

Agnetta, G. et al., Nucl. Instr. and Meth., **A 381**, 64, 1996.

Comedi, "Linux control and measurement device interface", http://stm.lbl.gov/comedi/, 2001.

ROOT, "An Object-Oriented Data Analysis Framework", http://root.cern.ch/, 2001.

Klett, J. D., "Stable analytical inversion solution for processing lidar returns", Appl. Opt. **20**, 211–220, 1985.

Klett, J. D., "Lidar inversion with variable backscatter extinction rations", Appl. Opt. **24**, 1638–1643, 1985.

Fenn, R. W. , "Correlation between atmospheric backscattering and meteorological visual range", Appl. Opt. **5**, 615–616, 1966.

Twomey, S. and Howell, H. B. , "Relative merit of white and monochromatic light for the determination of visibility by backscattering measurements", Appl. Opt. **4**, 501–506, 1965.